Applied Catalysis B: Environmental 245 (2019) 62–70

Contents lists available at ScienceDirect

Applied Catalysis B: Environmental

journal homepage: www.elsevier.com/locate/apcatb

Gas-phase dehydration of tetrahydrofurfuryl alcohol to dihydropyran over γ-Al_2O_3

Ling Li[a,b,1], Kevin J. Barnett[a,1], Daniel J. McClelland[a], Dongting Zhao[a], Guozhu Liu[b], George W. Huber[a,*]

[a] Department of Chemical and Biological Engineering, University of Wisconsin-Madison, Madison, WI, 53706, United States
[b] Key Laboratory for Green Chemical Technology of Ministry of Education, School of Chemical Engineering and Technology, Tianjin University, Tianjin 300072, PR China

ARTICLE INFO

Keywords:
Dehydration
Tetrahydrofurfuryl alcohol
Kinetics
Mechanism

ABSTRACT

Gas-phase dehydration of tetrahydrofurfuryl alcohol (THFA) to 3,4-2H-dihydropyran (DHP) was studied over solid acid catalysts. A γ-Al_2O_3 catalyst resulted in 90% DHP yield from THFA. The γ-Al_2O_3 deactivated due to solid coke formation but was nearly fully re-generable upon a high temperature calcination step (only 2.5% activity loss after 3rd regeneration). The high catalytic activity and selectivity of γ-Al_2O_3 was correlated to its high Lewis to Brϕnsted acid site ratio, as confirmed by ammonia temperature-programmed desorption (NH_3-TPD) and isopropylamine temperature-programmed desorption (IPA-TPD). Based on isotopic-labelling studies, a reaction mechanism was proposed in which THFA initially dehydrates into a carbenium intermediate prior to Wagner-Meerwien rearrangement into DHP. A kinetic model of THFA dehydration over γ-Al_2O_3 was developed according to kinetic experimental data. The best-fit model suggested the rate-determining step was the surface reaction of adsorbed THFA dissociating into adsorbed DHP and water.

1. Introduction

Synthesis of high value commodity chemicals from biomass has attracted considerable interest due to improved economics and the potential to lower the cost of biofuel production. Furfural is by volume one of the largest biomass based chemicals produced today, with over 600 ktons of capacity available worldwide [1]. Furfural can be hydrogenated into tetrahydrofurfuryl alcohol (THFA) in the vapor phase [2]. The gas phase dehydration of THFA over Al_2O_3 produces 3,4-2H-dihydropyran (DHP) [3–5]. DHP is known as a protection reagent of alcohol and phenols [6,7], in for example the syntheses of testosterone acyl esters [8]. Our group has previously reported that DHP is an important intermediate in the dehydration-hydration-hydrogenation (DHH) process to obtain 1,5-pentandediol (1,5-PD) from THFA [9–11]. Paul et al. [12] first reported that the dehydration of THFA over alumina produced DHP. Kline et al. [13] investigated the THFA dehydration over alumina at 623 K and reported DHP yields of 70%. Yamada et al. [14] studied alumina modified with Cu in THFA dehydration and observed improve catalytic stability and high DHP selectivity when adding hydrogen flow. In our previous research, DHP yields of 86% were achieved in gas-phase THFA dehydration over γ-Al_2O_3 at 648 K [11].

Since the 1960s, there have been multiple studies on the mechanism of THFA dehydration over γ-Al_2O_3. Gensler et al. proposed that the mechanism of THFA dehydration may proceed via a Wagner-Meerwein rearrangement reaction. In their research, ^{14}C-labelled THFA was dehydrated over γ-Al_2O_3 and the ^{14}C was found in 2- and 6-position of DHP (see Scheme 1). This conclusion was based on the distribution of products following oxidation of the ^{14}C labeled DHP product by O_3 or nitric acid [15]. Butler's group reported that 2-methylenetetrahydrofuran did not isomerize to DHP under the same condition as the THFA dehydration reaction. Therefore, they believed that 2-methylenetetrahydrofuran was not an intermediate in THFA dehydration [16]. Schwarz et al. studied the THFA dehydration using ^{13}C-labelled precursors in combination with collisional activation mass spectrometry. According to their results, the ring-enlargement was derived from a ring-enlarged oxonium ion [17]. These mechanisms suggest a diversity of possible pathways in this dehydration process.

The objective of this paper is to gain insights into the kinetics and mechanism of THFA dehydration reaction over γ-Al_2O_3 catalyst in gas phase. Little work has been performed to date in studying the active sites in this dehydration reaction. The surface properties of solid acid

* Corresponding author.
E-mail address: gwhuber@wisc.edu (G.W. Huber).
[1] These authors contributed equally to this work.

https://doi.org/10.1016/j.apcatb.2018.12.039
Received 9 August 2018; Received in revised form 10 December 2018; Accepted 15 December 2018
Available online 17 December 2018

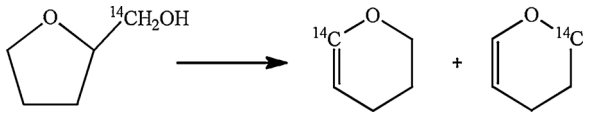

Scheme 1. ^{14}C labelled THFA dehydration reaction in reference [15].

catalysts were characterized, a mechanism was proposed based on the isotopic analysis, and a kinetic rate law was derived from the mechanism and fit to the experimental data. The results of this paper will allow us to develop a fundamental understanding of the underlying chemistry of this dehydration reaction and provide directions for designing improved catalytic systems.

2. Experimental section

2.1. Materials

NH_4^+-ZSM-5 (SiO_2/Al_2O_3 = 30), NH_4^+-Beta (SiO_2/Al_2O_3 = 25), and NH_4^+-Y (SiO_2/Al_2O_3 = 30) were purchased from Zeolyst International. γ- Al_2O_3 was purchased from Strem Chemicals. THFA (99%, Sigma-Aldrich), DHP (95%, AK Scientific), 3,6-Dihydro-2H-Pyran (96%, AK Scientific), and D-[1-^{13}C]xylose (100%, Omicron Biochemicals, Inc.) were used in this research.

2.2. Catalyst preparation

All catalysts were crushed and sieved to 45–80 mesh. The catalysts were pretreated in flowing He at 673 K for 1 h before the reaction. NH_4^+-ZSM-5, NH_4^+-Beta, NH_4^+-Y catalyst were calcined in a muffle furnace at 773 K for 4 h to convert to their hydrogen form prior to reaction tests.

2.3. Catalyst characterization

Ammonia temperature-programmed desorption (NH_3-TPD) and isopropylamine temperature-programmed desorption (IPA-TPD) were performed in a Micrometrics Autochem II 2920 instrument to obtain the total acid sites and Brϕnsted acid sites. Comparing the kinetic diameter of the THFA reactant (5.7 Å) to the channel and pore diameters of the catalysts tested suggests that the THFA can access all of the acid sites as determined by NH_3- and IPA-TPD. Approximately 100 mg of the sample was packed in a quartz cell and pretreated at 673 K for 1 h in He. For NH_3-TPD, the sample was saturated with 15% NH_3/He at 423 K for 1 h, and then flushed with He for 30 min to remove the physical adsorption of ammonia. The TPD process was performed by heating the sample at the rate of 10 K·min^{-1} from 423 K to 973 K under flowing He. The amount of ammonia desorbed was calculated by integrating the thermal conductivity detector (TCD) signal. For IPA-TPD, the IPA was injected in pulses into the sample at 323 K until saturation, and then the sample was purged with He for 1 h. In the IPA-TPD process, propene - which decomposes from IPA - was quantified using an online mass spectrometer to determine the Brϕnsted acid site density.

2.4. Nuclear magnetic resonance

Quantitative ^{13}C nuclear magnetic resonance (NMR) experiments were performed with ^{13}C isotopically labeled xylose. A Bruker Biospin (Billerica, MA) AVANCE III 500 MHz spectrometer fitted with a DCH (^{13}C-optimized) cryoprobe was used to analyze the samples with the Bruker standard pulse sequence 'zgig30' and the following parameters: an inter-scan relaxation delay of 15 s, a sweep width of 240 ppm centered at 110 ppm, and an acquisition time of 1 s with 59,520 data points and 128 scans. Before the test, Deuterium oxide (D_2O) was added to the sample (1:9 v/v) for the analyses. Mestrelab Research's MestReNova software was used to process the spectra.

2.5. Catalytic experiments

THFA dehydration reaction studies were carried out in a down-flow fixed bed reactor with γ-Al_2O_3 or zeolite catalysts at 101.3 kPa. The 1/4 OD stainless steel tube was loaded with catalyst and secured in a tube furnace comprised of aluminum blocks, heating tape, and insulation. The catalysts were pretreated in flowing He (40 ml/min, Airgas, industrial grade) at 673 K for 1 h prior to the reaction, except for the studies outlined in Section 3.3, in which different pretreatment temperatures were employed. The reactor was cooled to the reaction temperature following the pretreatment step. The feed (Tetrahydrofurfuryl alcohol, 99%) was pumped into the reactor with an HPLC pump (Varian Prostar 210 Series). Helium gas, DHP, and/or H2O were co-fed into the reactor for the kinetic studies in Section 3.5 to measure the reaction rate as a function of the concentration of the reactants and products (see Table S1). The vapor phase reactor effluent was passed through a dry ice + acetone bath condenser. The collected liquid samples were analyzed by gas chromatography (Shimadzu GC 2010 equipped with a flame ionization detector (FID) and a RTX-VMS column).

3. Results and discussion

3.1. THFA dehydration over various solid acids

The THFA dehydration reaction was investigated over a series of solid acid catalysts. DHP was the main product for all of the catalysts studied. Fig. 1 shows that H-Beta, H-Y, and H-ZSM-5 zeolite catalysts all gave similar DHP selectivity (53–61%). H-Beta was roughly two times more active than the other zeolites, with a THFA conversion of 24% (versus 15% and 12% for H-Y and H-ZSM-5, respectively). Notably, a 90% DHP selectivity at 70% THFA conversion was achieved over γ-Al_2O_3, making it the most active and selective of all the catalysts studied.

DHP formation turnover frequencies (TOF) were obtained by normalizing the specific rates with the Lewis acid site densities, as shown in Table 1. External and internal mass transfer limitations were shown not to exist based on Mears and Weisz-Prater criteria, as shown in Table S2. The Brϕnsted acid site (BAS) and Lewis acid site (LAS) densities calculated using IPA-TPD and NH_3-TPD, respectively are listed in Table 1. We observed that the LAS of the H-form zeolites increased in the same order (H-Y < H-ZSM-5 < H-Beta) as the DHP selectivity (Fig. 1), showing that the DHP selectivity rises with an increase in Lewis to Brϕnsted acid site ratio. Moreover, the Lewis acid site density for γ-Al_2O_3 was 0.34 mmol/g with few Brϕnsted acid sites (0.09 mmol/g)

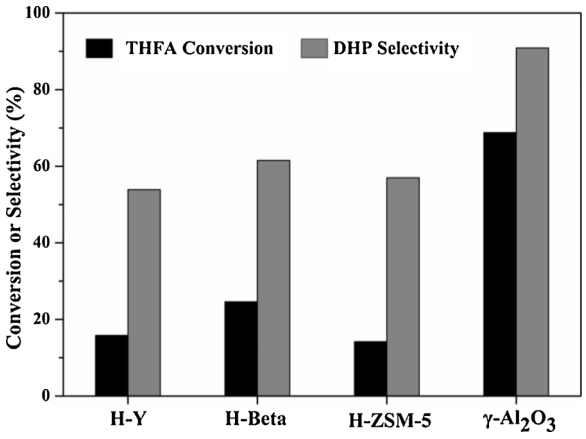

Fig. 1. Gas-phase THFA dehydration over various solid acid catalysts after 12 h TOS in a continuous flow reactor. Reaction conditions: T = 623 K, P = 101.3 kPa, P_{THFA} = 48.3 kPa, 0.28 g catalyst, $WHSV_{(THFA)}$ = 9.0 h^{-1}, He flow = 10 mL/min.

Table 1
DHP formation rate per Lewis acid site and first-order deactivation constants over various solid acids[a].

Catalyst	BAS [b] (mmol/g)	LAS [c] (mmol/g)	Rate (mmol/g/h)	DHP TOF [d] (h^{-1})	$k_d \times 10^4$ [e] (h^{-1})
H-Y	0.67	0.23	7.15	31.1	5.6
H-Beta	0.80	0.47	12.78	27.2	2.9
H-ZSM-5	0.41	0.31	6.63	21.4	3.8
γ-Al_2O_3	0.09	0.34	>53.35[f]	>156.9[f]	3.2

[a]Conversion values for all data can be found in Fig. 1.
[b]Brϕnsted Acid Site (BAS) determined by IPA-TPD.
[c]Lewis Acid Site (LAS) determined by NH_3-TPD and IPA-TPD.
[d]$DHP\ TOF = \frac{R_{DHP\ formation\ rate}}{LAS}$.
[e]$k_d = \frac{R_2 - R_1}{T_2 - T_1}$ R_2 : DHP formation rate at T_2 time; R_1 : DHP formation rate at T_1 time.
[f]Conversion for this reaction was 70%, thus we are under-reporting the intrinsic rate and TOF here.

detected. This indicates that γ-Al_2O_3 contained predominantly Lewis acid sites, which is in accordance with the literature [18]. The predominantly Lewis acidic γ-Al_2O_3 exhibited the highest DHP selectivity (Fig. 1), which suggests that Lewis acid sites are likely the active sites for DHP formation in THFA dehydration reaction. In addition, nearly 80% DHP selectivity was achieved over a ZrO_2 catalyst at 648 K, providing further evidence catalysts with a high concentration of Lewis acidity are more selective to the DHP product. The TOF of γ-Al_2O_3 (156.9 h^{-1}) was five to seven times higher than other catalysts tested for THFA dehydration. As the reaction progressed, all of these solid acid catalysts underwent deactivation shown in the Fig. S1. The first-order deactivation constants (k_d) were calculated by plotting the DHP formation rate versus time on stream as shown in Table 1.

3.2. THFA dehydration over γ-Al_2O_3

Dehydration of THFA over γ-Al_2O_3 was investigated at a low space velocity to observe the product selectivity at high conversion. As seen in Fig. 2A, near 100% THFA conversion and 90% DHP yields were obtained at 648 K and atmospheric pressure over 36 h time-on-stream, which was in line with our previous results [11]. Solid coke formed on the catalyst at these conditions, as shown by TGA characterization of the spent catalyst in Fig. S2. We also investigated the THFA dehydration reaction at low conversion, as shown in Fig. 2B, to better observe the deactivation and regenerability of γ-Al_2O_3. The initial yield was not fully recovered after a calcination step at 773 K, which is likely due to a loss in γ-Al_2O_3 surface area (see Table S3 in SI). However, the initial activity was nearly fully regained with subsequent regenerations, with only a 2.5% loss in activity following the 3rd regeneration step.

3.3. Effect of pretreatment temperature

We studied THFA dehydration following activation of the catalyst at different temperatures in helium to test the effect of pretreatment temperatures on the catalytic activity. Fig. 3 shows the THFA conversion and DHP selectivity over Al_2O_3 catalysts treated at different temperatures. The TOF of DHP formation and BAS/LAS density for Al_2O_3 catalysts subjected to different pretreatment regiments is shown in Table 2. The We observed that the Al_2O_3 without pretreatment exhibited around 17% THFA conversion and 75% DHP selectivity, while the catalyst treated at 673 K showed around 25% THFA conversion and

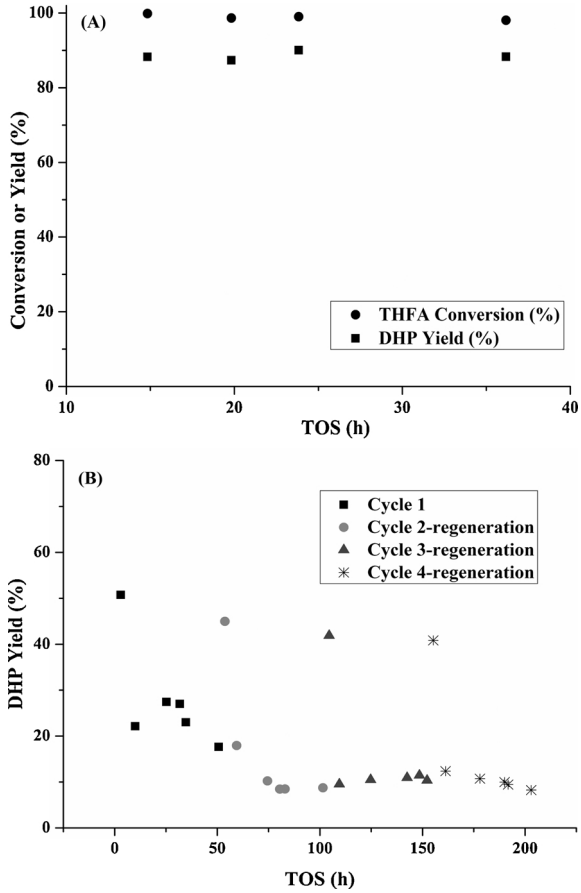

Fig. 2. THFA conversion and DHP yield versus time-on-stream over γ-Al_2O_3 in a continuous flow reactor. (A) High THFA conversion. Reaction conditions: T = 648 K, P = 101.3 kPa, P_{THFA} = 48.3 kPa, 0.46 g catalyst, $WHSV_{(THFA)}$ = 5.5 h^{-1}, He flow = 10 mL/min; (B) Low THFA conversion. Reaction conditions: T = 648 K, P = 101.3 kPa, P_{THFA} = 48.3 kPa, 0.028 g catalyst, $WHSV_{(THFA)}$ = 90 h^{-1}, He flow = 10 mL/min; Cycle 1: fresh γ-Al_2O_3; Cycle 2 : regenerated cycle 1 spent γ-Al_2O_3; Cycle 3: regenerated cycle 2 spent γ-Al_2O_3; Cycle 4: regenerated cycle 3 spent γ-Al_2O_3; Regeneration condition: calcination in air (40 mL/min) at 773 K for 4 h.

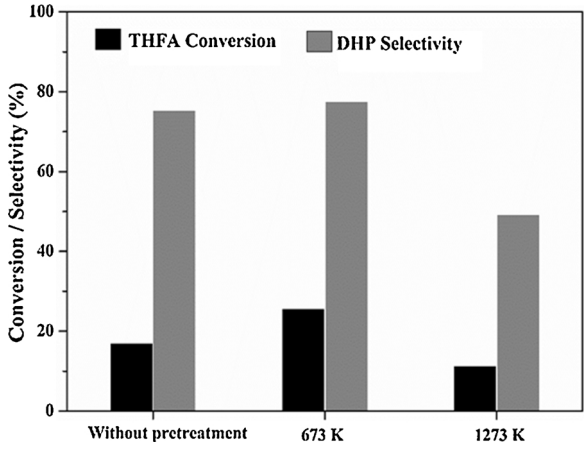

Fig. 3. THFA conversion and DHP selectivity over γ-Al_2O_3 at different pretreatment temperature after 25 h in a continuous flow reactor. Reaction conditions: T = 648 K, P = 101.3 kPa, P_{THFA} = 48.3 kPa, 0.028 g catalyst, $WHSV_{(THFA)}$ = 90 h^{-1}, He flow = 10 mL/min. Pretreatment conditions: 1 h, 40 mL/min He.

Table 2
DHP synthesis rate and DHP TOF over γ-Al_2O_3 after various pretreatments.

Catalyst sample	BAS[a] (mmol/g)	LAS[a] (mmol/g)	DHP TOF[a] (h^{-1})
SP	0.10	0.19	482.7
DP (673 K)	0.09	0.34	518.0
SP-DP	0.08	0.32	522.1
Without pretreatment	0.09	0.25	454.2
1273 K	0.04	0.13	381.7

[a] These data are calculated using the same method in Table 1. The conversion and reaction conditions for these catalysts can be found in the Figs. 3 and 4.

77% DHP selectivity. In combination with acid site density data (see Table 2), it is likely that this increase in activity may be associated with an increase in available Lewis acid sites. This result is in line with Digne et al. [19], who showed that the (100) facets of γ-Al_2O_3 were fully dehydrated at ~600 K, thus forming the coordinative unsaturated (penta-coordinate) aluminum ions, namely Lewis acid sites. Studies on the Lewis acidity of γ-Al_2O_3 showed that Lewis acid sites, in the form of coordinatively unsaturated aluminum ions, were generated after dehydration/dehydroxylation of the surface [20]. Sautet et al. [21] concluded that the distribution of the coordination number of surface aluminum sites depend on the pretreatment temperature. In contrast, the values of THFA conversion (~11%) and DHP selectivity (~ 49%) for the Al_2O_3 catalyst treated at 1273 K were lower than the same catalyst treated at 673 K, which is likely due to the decline in Lewis acid sites (see Table 2). The γ-Al_2O_3 treated at high temperature likely resulted in mixture of θ-γ-Al_2O_3 and α-Al_2O_3. This phase transition has been shown to lower the Lewis acid site density [22], which is consistent with our results (Table 2).

3.4. Effect of steam exposure on γ-Al_2O_3

The γ-Al_2O_3 catalyst was steam pretreated and tested for THFA dehydration to study the effect that the steam generated during the dehydration reaction may have on the active sites and product selectivity. Fig. 4 compares the THFA conversion and DHP selectivity over steam treated γ-Al_2O_3 (SP-Al_2O_3), dry He treated γ-Al_2O_3 (DP-Al_2O_3), and steam treated followed by dry He treated γ-Al_2O_3 (SP-DP-Al_2O_3), respectively. We observed that the SP-Al_2O_3 catalyst exhibited around 17% THFA conversion and 58% DHP selectivity, while the DP-Al_2O_3 catalyst gave around 25% THFA conversion and a much higher DHP selectivity of 77%. Literature has reported that the presence of water

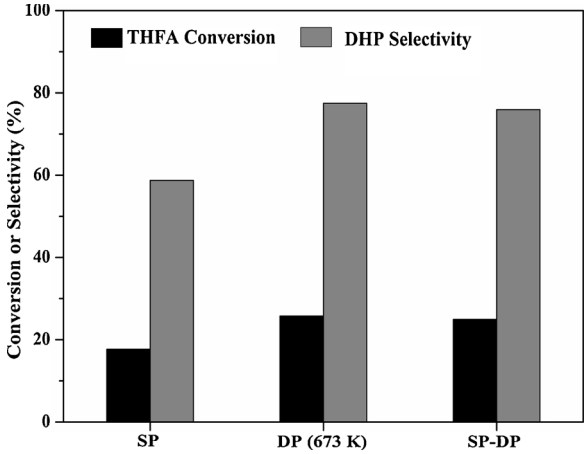

Fig. 4. THFA conversion and DHP selectivity over γ-Al_2O_3 at various steam pretreatment condition after 25 h in a continuous flow reactor. Reaction condition: T = 648 K, P = 101.3 kPa, P_{THFA} = 48.3 kPa, 0.028 g catalyst, $WHSV_{(THFA)}$ = 90 h^{-1}, He flow = 10 ml/min. SP: Steam pretreatment; DP: Dry pretreatment in He; SP-DP: Steam pretreatment – Dry pretreatment regeneration. Pretreatment conditions: 673 K, 1 h, 40 ml/min He (0.04 ml/min H_2O for SP).

has resulted in significant reduction of the surface Lewis acidity of γ-Al_2O_3 [23]. Wischert et al. [21] demonstrated that water preferentially disassociates on the highly under-coordinated aluminum atoms regarded as Lewis acid sites to form surface hydroxyl species. Roy et al. [24] found that the amount of 2-propanol adsorbed on the surface γ-Al_2O_3 sample with prior exposure to water was 73% lower than the value over γ-Al_2O_3 without any prior water exposure. Interestingly, the performance of SP-DP-Al_2O_3 (THFA conversion ~25% and DHP selectivity ~75%) was very similar with the DP-Al_2O_3 catalyst, indicating water poisoning is a regenerable deactivation mechanism. This is consistent with the work of DeWilde et al. who observed that the rate of ethylene and diethyl ether formation rate from ethanol dehydration decreased over the γ-Al_2O_3 catalyst treated in water prior to reaction, but that the rate of ethylene and diethyl ether formation recovered to similar values upon treatment of the water exposed catalyst at 723 K for 4 h [25]. We infer that water simply blocks adsorption sites on the γ-Al_2O_3 surface rather than destroying the active sites.

3.5. Kinetics of THFA dehydration

Partial pressures of THFA, DHP, and water were varied in the feed stream to develop a kinetic model based on the three main species present in THFA dehydration. A positive order dependence (~ 0.5) in THFA partial pressure (THFA partial pressure = 5–15 kPa) was observed for the THFA consumption rate over γ-Al_2O_3, as shown in Fig. 5A. Negative dependences for THFA consumption rate were found for the partial pressures of DHP and water over γ-Al_2O_3 (Fig. 5B, C). A kinetic model employing Hougen-Watson (HW) kinetics was constructed. In the model, we assumed that surface reaction was the rate-determining step and other steps were in quasi-equilibrium. The first step (Eq (1)) is the reversible adsorption of THFA ($C_5H_{10}O_2$) onto the Al_2O_3 surface. The adsorbed THFA adsorbs to second vacant site and dissociates to form adsorbed DHP (C_5H_8O) and H_2O as shown in Eq. 2. This surface reaction step can be separated into two steps: i) dehydration of the THFA alcohol group and ii) isomerization of the furan ring to DHP, but is only considered as a single step for the purposes of the kinetic model. The final steps involve desorption of adsorbed DHP and H_2O species as shown in Eqs. 3 and 4, respectively. Based on these assumptions, the kinetic model shown in Eq. 5 was derived.

$$C_5H_{10}O_2 + S \leftrightarrow C_5H_{10}O_{2\,ads} \quad (1)$$

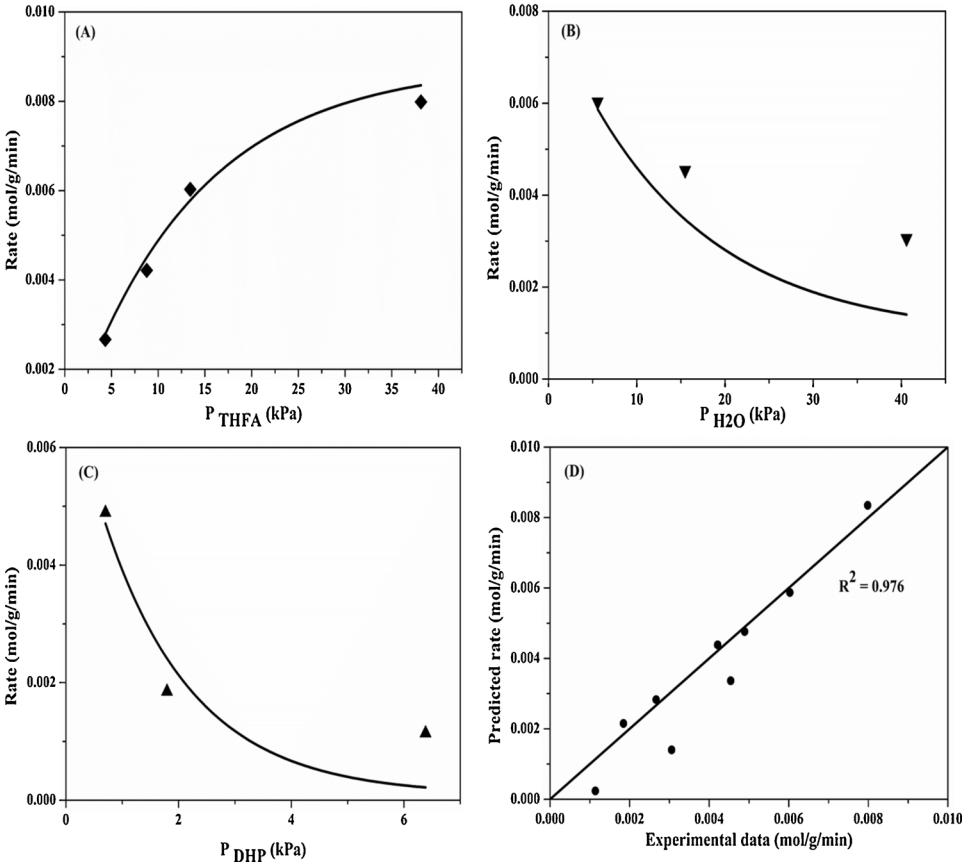

Fig. 5. THFA consumption rates for THFA dehydration over γ-Al_2O_3 as a function of partial pressure. (A) As a function of THFA partial pressure (P_{H2O} = 5.05 kPa, P_{DHP} = 0.00 kPa). (B) As a function of H_2O partial pressure (P_{THFA} = 15.15 kPa, P_{DHP} = 0.00 kPa). (C) As a function of DHP partial pressure (P_{THFA} = 15.15 kPa P_{H2O} = 0.00 kPa). (D) Parity plot for the kinetics model in eqn (5). Note: Inlet partial pressuresm the resulting conversion and reaction rate data are given in Table S1.

$$C_5H_{10}O_{2\,ads} + S \rightarrow C_5H_8O_{ads} + H_2O_{ads} \quad (2)$$

$$C_5H_8O_{ads} \leftrightarrow C_5H_8O + S \quad (3)$$

$$H_2O_{ads} \leftrightarrow H_2O + S \quad (4)$$

$$r = \frac{k_r K_1 P_{THFA}}{(1 + K_1 P_{THFA} + K_3 P_{DHP} + K_4 P_{H_2O})^2} \quad (5)$$

$$R^2 = 1 - \frac{\sum_{i=1}^{n} (r_{experimental} - r_{model})^2}{\sum_{i=1}^{n} r_{experimental}^2} \quad (6)$$

In Eq. 5, k_r is the rate constant of the rate limiting step, while K_1, K_3, and K_4 are the equilibrium constants of THFA adsorption, DHP desorption, and H_2O desorption, respectively. The kinetic parameters were estimated using the data presented in Fig. 5 and are listed in Table 3. The best-fit HW model is based on the minimization of the least squares error shown in Eq. 6, where 'r' is the consumption rate of THFA and 'n' is the number of experimental data points. The solid lines shown in Fig. 5 represent fit data using Eq. 5 in Matlab software.

The kinetics model fit results as a function of THFA partial pressure, H_2O partial pressure, and DHP partial pressure are shown in Fig. 5A–C respectively. Helium gas, DHP, and/or H2O were co-fed into the reactor to control the concentration of reactants and products while measuring the rate of reaction in Fig. 5. Details on the inlet partial pressures, conversion and rates reported in Fig. 5 are given in Table S1. The parity plot shown in Fig. 5D, shows the variance between the experimental data and kinetic model. An Akaike Information Criterion (AIC) analysis performed on the L-H model in Eq. 5 showed that all four kinetic parameters (k_r, K1, K3, and K4) were essential to the model and that the downselected model is much preferred to other models (with fewer parameters) we tested in this study (see Table S4 for more details).

Table 3
Estimated kinetic parameters for THFA dehydration over γ-Al_2O_3 using the model presented in Eq. (3) and data from Fig. 5.

Catalyst	K_1	K_3	K_4	k_r (mol/g/min/kPa)
γ-Al_2O_3	0.90 ± 0.19	32.05 ± 4.67	0.35 ± 0.29	13.21 ± 1.56

Christopher et al. [26] reported that DHP can further dehydrate to hydrocarbons above 573 K and DHP can decompose into acrolein and ethylene over γ-Al_2O_3 catalyst above 673 K. We observed only small amounts of acrolein (< 0.2% selectivity) in the THFA dehydration products. The H_2O desorption equilibrium constant obtained from the model (K_4 in Table 3) is ~3 times lower than THFA adsorption equilibrium and ~90 times lower than DHP desorption equilibrium constant suggesting strong adsorption of water to the catalyst surface and possible inhibition of THFA dehydration by site blocking.

3.6. Proposed mechanism of THFA dehydration

A reaction scheme for THFA dehydration process based on the experimental work in this paper is proposed in Scheme 2. Initially, THFA adsorbs onto a Lewis acid site of γ-Al_2O_3 (Step 1). The adsorbed THFA then dehydrates into adsorbed water and a carbenium ion (Step 2 and 3). The carbenium then re-arranges to form absorbed DHP (Steps 4 & 5). Finally, the adsorbed DHP and H_2O desorb from the γ-Al_2O_3 (Steps 6 & 7). We will now justify this reaction mechanism using isotopic labeling.

3.7. Mechanism of THFA dehydration: isotopic labelling studies

The surface reaction of THFA dehydration includes two steps: i) formation of a tetrahydrofurfuryl carbenium ion and ii) carbenium ion rearrangement, as shown in Schemes 3A and B, respectively. Butler et al. [16] hypothesized that a tetrahydrofurfuryl carbenium ion was generated by removal of the exocyclic hydroxyl group via the acid sites

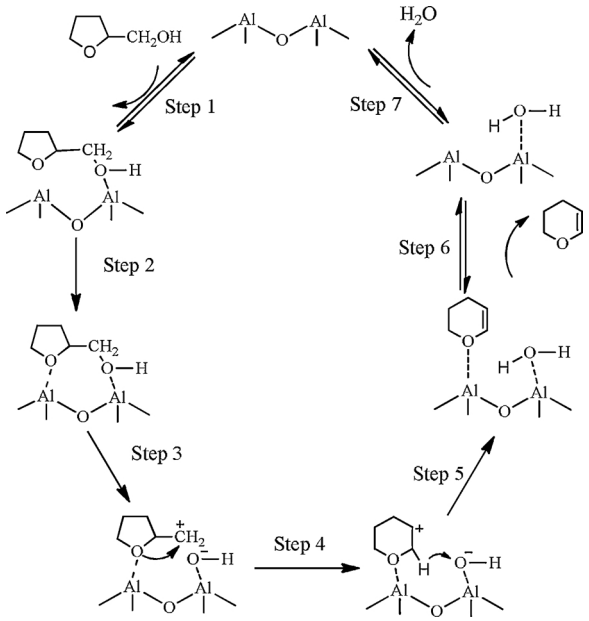

Scheme 2. Proposed reaction network for THFA dehydration to DHP over γ-Al_2O_3.

of γ-Al_2O_3 since DHP was the major product from both tetrahydrofurfuryl acetate and 2-methoxymethyltetrahydrofuran. Wilson et al. [26] proposed that the THFA dehydration step progressed through a furfuryl cation rather than a radical.

We propose the transformation of tetrahydrofurfuryl into DHP involves carbenium chemistry. Both tertiary and secondary carbenium ions are more stable than a primary carbenium [27]. Since the tetrahydrofurfuryl carbenium ion formed following dehydration of the alcohol group is a primary carbenium ion, the rearrangement to DHP proceeds through a more stable secondary or tertiary carbenium ion. Butler et al. [16] proposed a tertiary tetrahydrofurfuryal carbenium ion was involved in conversion of THFA and DHP. This tertiary carbenium ion would produce cyclopyl methyl ketone, as shown in Pathway A in Scheme 3. However, the cyclopyl methyl ketone was not observed in our experiments, indicating that this rearrangement pathway does not occur.

There are two possible pathways that involve a secondary carbenium ion. In Pathway B (see Scheme 3), the α-C should relocate to the DHP 5-position through the cleavage and formation of a C—C bond during rearrangement reaction. Pathway C results in the α-C at the 6-position of DHP via the cleavage and formation of C–O bond during the rearrangement step.

^{13}C isotopic-labelled experiments were performed to investigate the rearrangement pathways of the tetrahydrofurfuryl carbenium ion in THFA dehydration. ^{13}C THFA isotopically-labelled at the exocyclic carbon atom was prepared by dehydration of D-xylose with ^{13}C at the 1-position, followed by hydrogenation of the resulting ^{13}C furfural to THFA. The detailed preparation process for the ^{13}C labeled THFA and DHP is shown in Scheme S1. The ^{13}C THFA dehydration products containing the ^{13}C isotope were analyzed by NMR, which is shown in Fig. 6.

The quantitative ^{13}C NMR spectrum of a DHP standard is shown in Fig. 6A. Fig. 6B shows the quantitative ^{13}C NMR spectrum of ^{13}C labeled products from ^{13}C labelled THFA derived from ^{13}C labelled xylose. The NMR signal at 144.3 ppm is the ^{13}C at the DHP 6-carbon position, indicating that Pathway C shown in Scheme 2 is the favorable pathway of this rearrangement. No ^{13}C peaks were observed at 23.0 ppm, 19.7 ppm, or 100.7 ppm, meaning that no ^{13}C was located at the 3-, 4-, and 5-positions of DHP. There were many unidentified peaks in NMR spectrum, most notably between 20–40 ppm and at 132.5 ppm. These peaks are attributed to products from xylose dehydration or furfural hydrogenation due to incomplete conversion and separation of xylose and furfural. Furthermore, these peaks did not match those of hypothesized side products of THFA dehydration, including xylose, furfural, furfuryl alcohol, tetrahydrofurfuryl alcohol, and 3,6-Dihydro-2H-pyran.

Interestingly, a ^{13}C peak at 65.8 ppm ascribed to DHP 2-position was also observed in the NMR spectrum, which is consistent with the findings of Walter et al [15]. Moreover, the ratio of ^{13}C in 6- and 2-position was roughly 1:0.9, suggesting that the amount of ^{13}C in the 6-

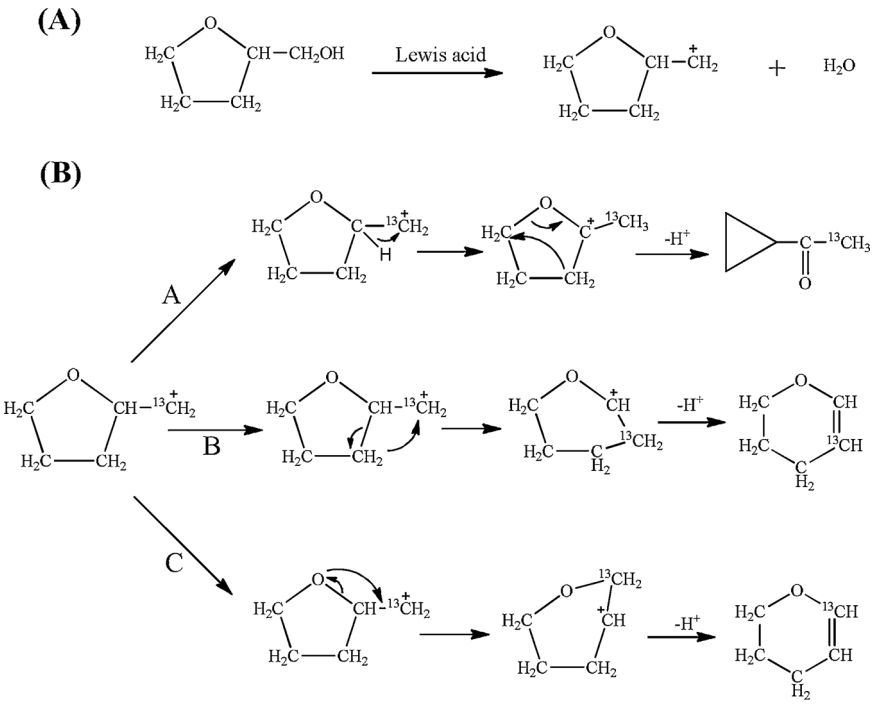

Scheme 3. (A) Hypothesized carbenium formation mechanism and (B) possible ring rearrangement pathways in THFA dehydration.

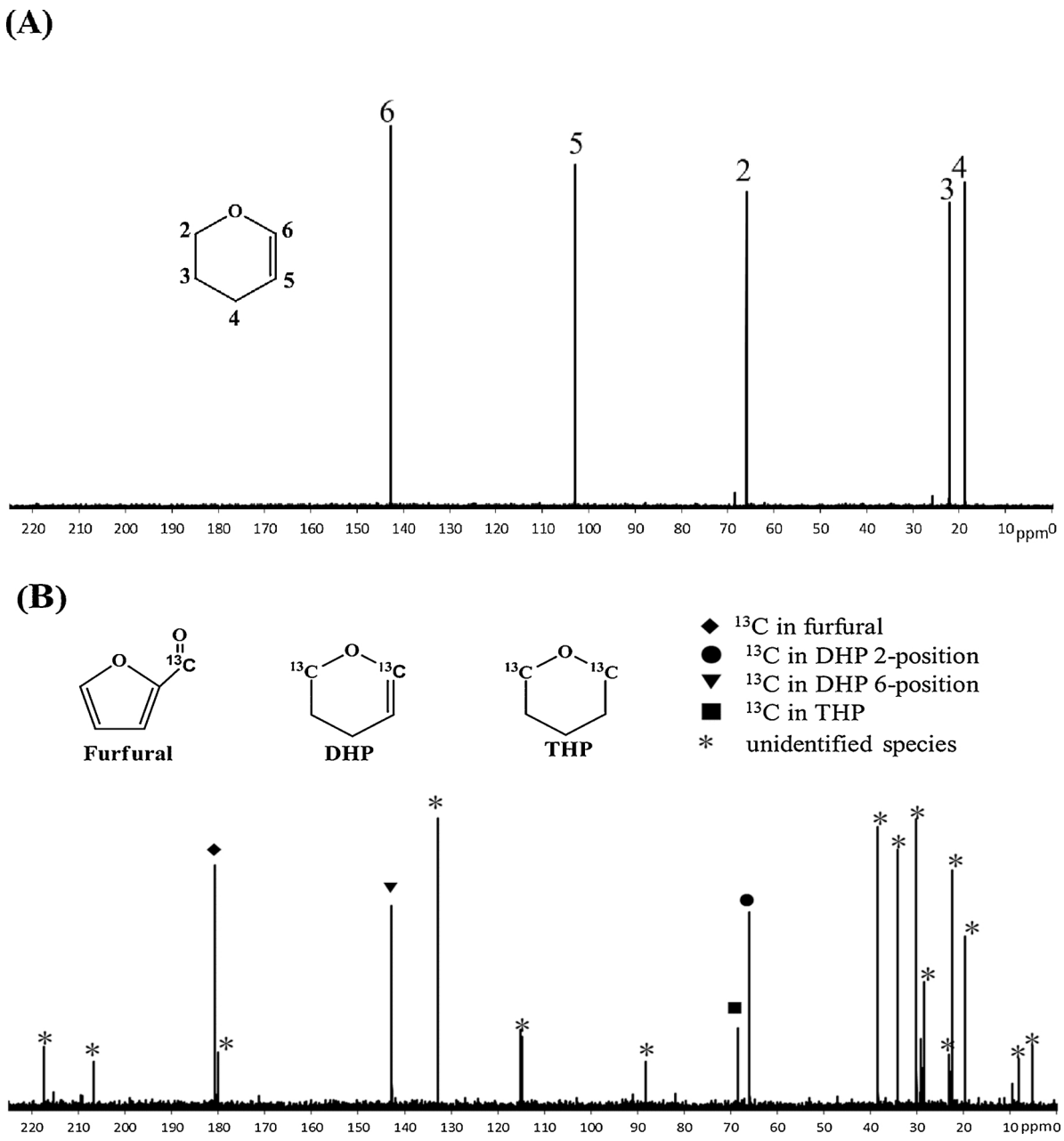

Fig. 6. Quantitative ^{13}C NMR spectra (A) pure DHP; (B) ^{13}C labelled products from ^{13}C labelled THFA derived from 0.5 wt % ^{13}C-labelled xylose in water solvent.

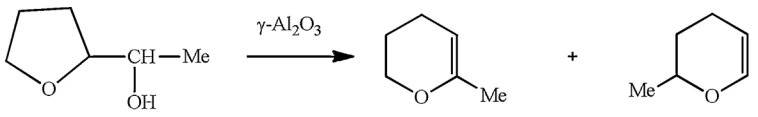

α-methyltetrahydrofurfuryl alcohol 6-methyldihydropyan 2-methyldihydropyan

Scheme 4. α-methyltetrahydrofurfuryl alcohol dehydration over γ-Al_2O_3 in reference.

and 2-position were almost identical. Therefore, there is an isomerization process occurring during the DHP formation. Walter et al. [28] reported that α-methyltetrahydrofurfuryl alcohol passed over alumina gives a mixture of 2-methyldihydropyran and 6-methyldihydropyan in products (see Scheme 4). There are two possibilities for DHP isomerization as shown in Scheme 5. Scheme 5A involves isomerization through the carbon ring with a series of reversible C = C shifts, while Scheme 5B involves isomerization through an oxocarbenium ion. It has been reported that γ-Al_2O_3 can catalyze n-butene skeletal isomerization to isobutene at 753 K [29]. In order to test the potential for isomerization process through the carbon ring (Scheme 5A), DHP was passed over γ-Al_2O_3 at THFA dehydration reaction, which is shown in the Supporting Information. In Fig. S4, 0.04% of 3,6-2H-dihydropyran yield is observed, indicating that DHP isomerization through Scheme 5A is not occurring.

Walter et al. [30] proposed that DHP in contact with alumina exchanges its oxygen atoms, as well as the hydrogen atoms at the 3- and 5-position of DHP. Schultz et al. [31] proposed aryloxygenones give dihydrofurans through oxocarbenium ions in arylation reaction. Thomas et al [32].reported the glycosyl oxocarbenium ions by Infrared Ion

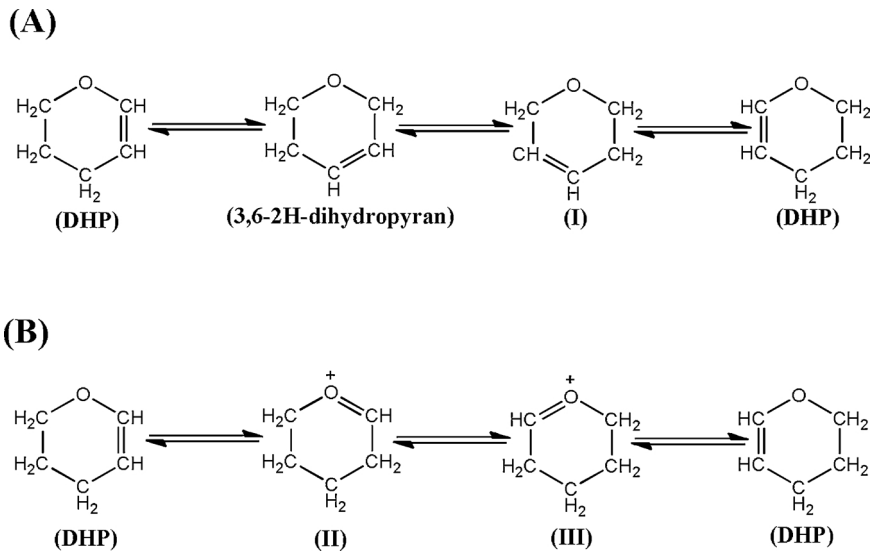

Scheme 5. Possible pathways for 2–6 scrambling in DHP.

Spectroscopy. Moreover, Woodward proposed the key step in the isomerization of steroidal sapogenins is a reversible hydride transfer involving the oxonium compounds [33]. Stein et al. studied the hydride shifts in DHP reaction over Al_2O_3 by isotopic study and kinetics [34]. Here we propose a possible isomerization pathway involving oxocarbenium ion, which was depicted in Scheme 5B. This isomerization process occurs via the formation of oxocarbenium II (Scheme 5B), which undergoes the hydride shift to form DHP.

4. Conclusions

DHP yields of 90% were achieved over γ-Al_2O_3 at full THFA conversion. Moreover, γ-Al_2O_3 was able to be regenerated to more than 90% of its initial activity after four reaction-regeneration cycles. Lewis acid sites were found to be the active catalytic sites based on the catalyst acid site characterization. There was a 5–7 times higher in TOF of DHP formation with γ-Al_2O_3 than for zeolite acid catalysts. The THFA dehydration mechanism likely involves the formation of a carbenium ion followed by carbenium-rearrangement. A rearrangement pathway starting with the cleavage of the heterocyclic C–O bond was proposed based on ^{13}C-labelled isotopic studies. ^{13}C-labelled in 2-position of DHP was observed, likely due to 2–6 scrambling in DHP via an oxocarbenium intermediate. A positive order dependence (~ 0.5) in THFA partial pressure and negative dependences in DHP and H_2O partial pressures were observed for the THFA consumption rate over γ-Al_2O_3. A kinetic model based off the experimental data suggests the rate-limiting step is the surface reaction involving adsorbed THFA dissociation to adsorbed DHP and H_2O.

Author contributions

Ling Li and Kevin J. Barnett contributed equally.

Acknowledgements

This work was funded by the Department of Energy, Office of Energy Efficiency Renewable Energy (EERE), under Award Number DE-EE0006878. Any opinions, findings, and conclusions or recommendations expressed in this materials are those of the authors and do not necessarily reflect the view of the department of Energy. We thank Siddarth H. Krishna for assistance with ^{13}C-labelled experiments.

Appendix A. Supplementary data

Supplementary material related to this article can be found, in the online version, at doi:https://doi.org/10.1016/j.apcatb.2018.12.039.

References

[1] R. Mariscal, P. Maireles-Torres, M. Ojeda, I. Sádaba, M. López Granados, Furfural: a renewable and versatile platform molecule for the synthesis of chemicals and fuels, Energy Environ. Sci. 9 (2016) 1144–1189.
[2] J.N. Chheda, G.W. Huber, J.A. Dumesic, Liquid-phase catalytic processing of biomass-derived oxygenated hydrocarbons to fuels and chemicals, Angew. Chem. Int. Ed. 46 (2007) 7164–7183.
[3] L.E. Schniepp, H.H. Geller, Preparation of Dihydropyran, 8-hydroxyvaleraldehyde and 1,5-pentanediol from tetrahydrofurfuryl alcohol, J. Am. Chem. Soc. 68 (1946) 1646.
[4] C.L. Wilson, Reactions of furan compounds. VIII. Dehydration of tetrahydrofurfuryl alcohol to 2,3-Dihydropyran and subsequent formation of acrolein and etheylene, J. Am. Chem. Soc. 69 (1947) 3004.
[5] O.W. Cass, Chemical intermediates from furfural, Ind. Eng. Chem. 40 (1948) 216–219.
[6] A.C. Ott, M.F. Murray, R.L. Pederson, The reaction of dihydropyran with steroidal alcohols. Utility in the syntheses of testosterone Acyl esters, J. Am. Chem. Soc. 1952 (1952) 1239–1241.
[7] F.B. Mueller, B.S. Brand, M.H. Sauter, L.F. Roehl, H.E. Ammermann, N.G. Lorenz, Dihydropyran derivatives and crop protection agents containing, US patent 5536734 (1994).
[8] A. Ott, M.A. Murray, R. Peders, The reaction of dihydropyran with steroidal alcohols. Utility in the syntheses of testosterone Acyl esters, J. Am. Chem. Soc. 74 (1952) 1239–1241.
[9] J. He, K. Huang, K.J. Barnett, S.H. Krishna, D.M. Alonso, Z.J. Brentzel, S.P. Burt, T. Walker, W.F. Banholzer, C.T. Maravelias, I. Hermans, J.A. Dumesic, G.W. Huber, New catalytic strategies for alpha,omega-diols production from lignocellulosic biomass, Faraday Discuss. 202 (2017) 247–267.
[10] K. Huang, Z.J. Brentzel, K.J. Barnett, J.A. Dumesic, G.W. Huber, C.T. Maravelias, Conversion of furfural to 1,5-pentanediol: process synthesis and analysis, ACS Sustain. Chem. Eng. (2017) 4699–4706.
[11] Z.J. Brentzel, K.J. Barnett, K. Huang, C.T. Maravelias, J.A. Dumesic, G.W. Huber, Chemicals from biomass: combining ring-opening tautomerization and hydrogenation reactions to produce 1,5-pentanediol from furfural, ChemSusChem 10 (2017) 1351–1355.
[12] R. Paul, Stability of the tetrhydrofuran ring. II. Dehydration of tetrahydrofurfuryl alcohol, Bull. Soc. Ckim. 53 (1933) 1489–1495.
[13] C.L. Kline, J. Turkbvich, Dehydration of tetrahydrofurfuryl alcohol, J. Am. Chem. Soc. 67 (1945) 498.
[14] S. Sato, J. Igarashi, Y. Yamada, Stable vapor-phase conversion of tetrahydrofurfuryl alcohol into 3,4-2H-dihydropyran, Appl.Catal. A 453 (2013) 213–218.
[15] W.J. Gensler, G.L. Mcleod, Fate of the carbinol in the conversion of tetrahydrofurfuryl alcohol to dihydropyran, J. Org. Chem. 28 (1963) 3194–3197.
[16] J.D. Butler, R.D. Laundon, Intermediates and products in the catalytic vapor phase dehydration and ammonolysis of 2-hydroxymethyltetrahydrofuran over alumina, J. Chem. Soc. C (1969) 173–176.
[17] H. Thies, R. Wolfschtz, G.F.J. Schmidt, H. Schwar, Mechanismus Der Protonkatalyslerten Gasphasendehydratisierung von furfurylalkohol, Tetrahedron

38 (1982) 1647–1656.
[18] J.A. Ripmeester, Surface acid site characterization by means of CP/MAS Nitrogen-15 NMR, J. Am. Soc. Chem. 105 (1983) 2925–2927.
[19] M. Digne, Use of DFT to achieve a rational understanding of acid-basic properties of γ-alumina surfaces, J. Catal. 226 (2004) 54–68.
[20] J.B. Peri, A model for the surface of γ-Alumina, J. Phy. Chem. 69 (1965) 220–230.
[21] R. Wischert, P. Laurent, C. Coperet, F. Delbecq, P. Sautet, Gamma-alumina: the essential and unexpected role of water for the structure, stability, and reactivity of "defect" sites, J. Am. Chem. Soc. 134 (2012) 14430–14449.
[22] G. Busca, Structural, surface, and catalytic properties of aluminas, Adv. Catal. 57 (2014) 319–404.
[23] Q. Dai, B. Yan, Y. Liang, B. Xu, Water effects on the acidic property of typical solid acid catalysts by 3,3-dimethylbut-1-ene isomerization and 2-propanol dehydration reactions, Catal. Today 295 (2017) 110–118.
[24] S. Roy, G. Mpourmpakis, D.-Y. Hong, D.G. Vlachos, A. Bhan, R.J. Gorte, Mechanistic study of alcohol dehydration on γ-Al2O_3, ACS Catal. 2 (2012) 1846–1853.
[25] J.F. DeWilde, H. Chiang, D.A. Hickman, C.R. Ho, A. Bhan, Kinetics and mechanism of ethanol dehydration on γ-Al_2O_3: the critical role of dimer inhibition, ACS Catal. 3 (2013) 798–807.
[26] C.L. Wilson, Reactions of furan compounds. VIII. Dehydration of tetrahydrofurfuryl alcohol to 2,3-dihydropyran and subsequent formation of acrolein and ethylene, J. Am. Chem. Soc. 69 (1947) 3004–3006.
[27] H. Pines, J. Manassen, The mechanism of dehydration of alcohols over alumina catalysts, Adv. Catal. 16 (1966) 49–93.
[28] Walter J. Gensler, Ieva Ruks, S. Marburg, Alumina-catalyzed Rearrangements of a-Methyltetrahydrofurfuryl Alcohol, 5-Methyltetrahydrofurfuryl Alcohol, 2-Methyl-2,3-dihydropyran, and 6-Methyl-2,3-dihydropyran, Chem. Commun. 21 (1966) 782–783.
[29] M. Trombetta, G. Busca, S.A. Rossini, V. Piccoli, U. Cornaro, FT-IR studies on light olefin skeletal isomerization catalysis, J. Catal. 168 (2007) 334–348.
[30] W.J. Gensler, P.T. Manos, I. Ruks, Hydrogen and oxygen exchange in Dihydropyan over hot alumina, J. Org. Chem. 33 (1968) 3408–3411.
[31] A.G. Schultz, R.D. Lucci, Heteroatom directed photoarylation. Photochemistry of aryloxyenones, J. Org. Chem. 40 (1975) 1371–1372.
[32] H. Elferink, M.E. Severijnen, J. Martens, R.A. Mensink, G. Berden, J. Oomens, F. Rutjes, A.M. Rijs, T.J. Boltje, Direct experimental characterization of glycosyl cations by infrared ion spectroscopy, J. Am. Chem. Soc. 140 (2018) 6034–6038.
[33] R.B. Woodward, F. Sondheimer, Y. Mazur, The mechanism of the isomerization of steroidal sapogenines at C-25, J. Am. Chem. Soc. 80 (1958) 6693–6694.
[34] S.H. Stein, Reaction of Isotopically Labelled Dihydropyran over Alumina, Dissertation (1967).